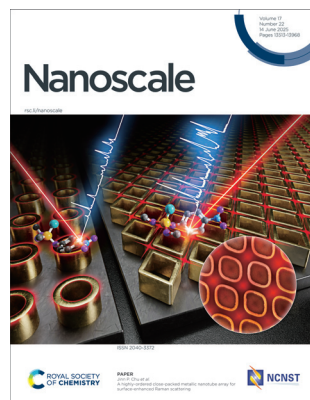


IN THIS ISSUE

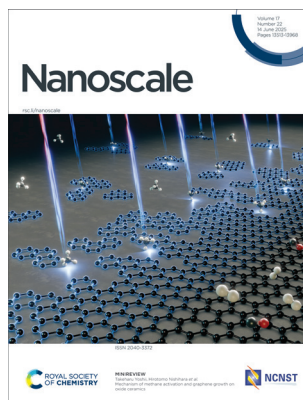
ISSN 2040-3372 CODEN NANOHL 17(22) 13513–13968 (2025)



Cover

See Jinn P. Chu *et al.*, pp. 13685–13697.

Image reproduced by permission of Jinn P. Chu from *Nanoscale*, 2025, **17**, 13685.



Inside cover

See Takeharu Yoshii, Hirotomo Nishihara *et al.*, pp. 13646–13652.

Image reproduced by permission of Takeharu Yoshii from *Nanoscale*, 2025, **17**, 13646.

EDITORIAL

13526

Chiral nanomaterials: theory, synthesis, applications and challenges

Nicholas A. Kotov,* Jeanne Crassous,* David B. Amabilino* and Pengfei Duan*

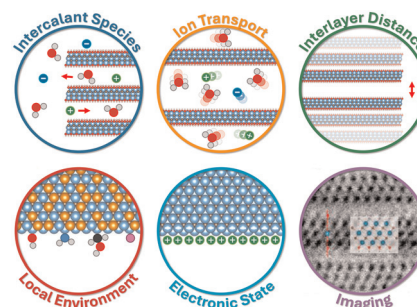


REVIEWS

13531

Material characterization methods for investigating charge storage processes in 2D and layered materials-based batteries and supercapacitors

Albert de Kogel, Ruocun (John) Wang,* Wan-Yu Tsai,* Maciej Tobis, Robert Leiter, Ruipeng Luo, Evan Wenbo Zhao,* Simon Fleischmann* and Xuehang Wang*



Environmental Science: Atmospheres

GOLD
OPEN
ACCESS

Connecting communities
and inspiring new ideas

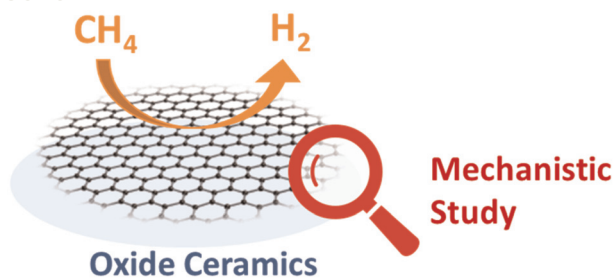
rsc.li/submittoEA

Fundamental questions
Elemental answers



MINIREVIEWS

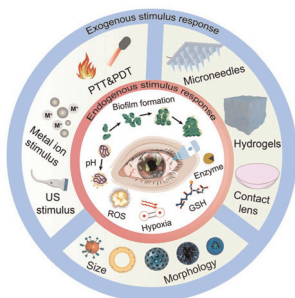
13646



Mechanism of methane activation and graphene growth on oxide ceramics

Hanzhang Zhou, Mengxuan Zhang, Takeharu Yoshii,*
Devis Di Tommaso and Hiroto Nishihara*

13653

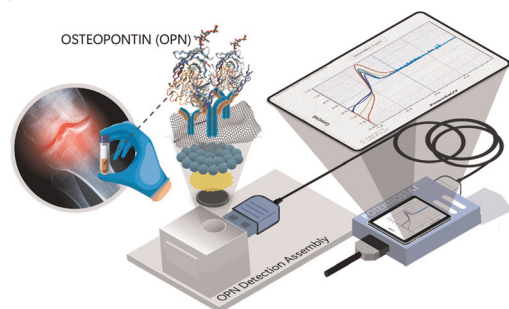


Stimulus-responsive nanomaterials for ocular antimicrobial therapy

Tao Zhang and Zichao Luo*

COMMUNICATION

13668

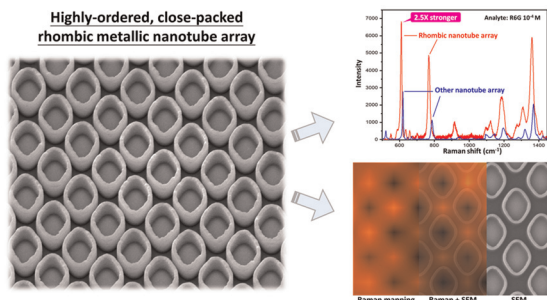


An electrochemically charged nanoengineered bioelectronic immunosensing device for osteopontin detection in serum samples

Daphika S. Dkhar, Supratim Mahapatra and
Pranjali Chandra*

PAPERS

13685



A highly-ordered close-packed metallic nanotube array for surface-enhanced Raman scattering

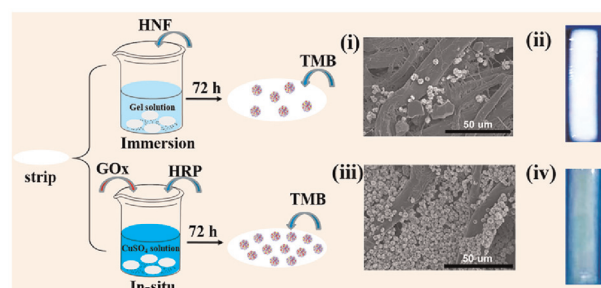
Ting-Hao Chang, Alfreda Krisna Altama,
Jun-Ting Wang, Pakman Yiu and Jinn P. Chu*



13698

In situ growth of enzyme-inorganic hybrid nanoflowers on paper strips for the visual detection of saliva-level glucose

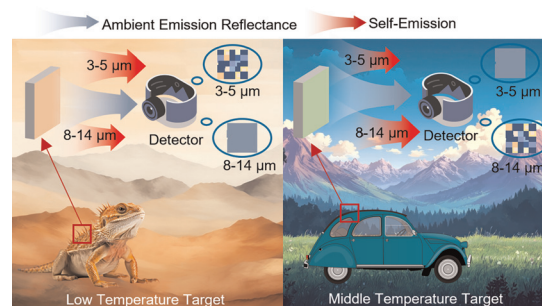
Zifeng Zhang,* Shiwen Wang, Tingjun Chen, Hui Wang* and Qian Dou*



13708

Tri-spectral decoupled programmable thermal emitter for multimode camouflage with heterogeneous phase-change integration

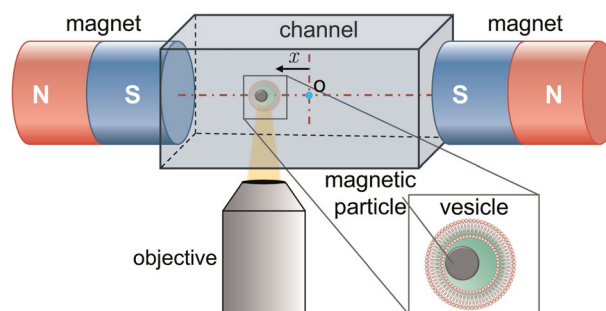
Sihong Zhou, Shikui Dong, Jiameng Song, Yanming Guo, Yong Shuai* and Guangwei Hu*



13720

Magnetically driven lipid vesicles for directed motion and light-triggered cargo release

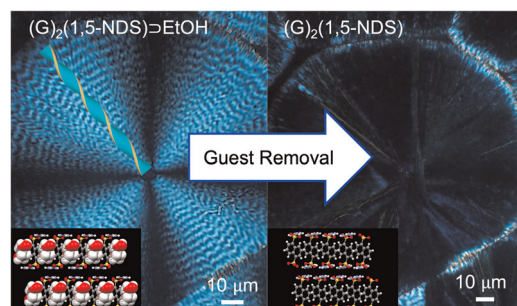
Vinit Kumar Malik, Chih-Tang Liao, Chenghao Xu, Abdallah Daddi-Moussa-Ider, On Shun Pak, Yuan-Nan Young and Jie Feng*



13727

Guest removal from ring-banded guanidinium organosulfonate hydrogen-bonded frameworks

Rochelle B. Spencer, Anna Yusov, Alexandra M. Dillon, Akash Tiwari, Oriol Arteaga, Sophia Sburlati, St. John Whittaker, Wantong Wu, Sixian Chen, Alexander G. Shtukenberg, Michael D. Ward,* Bart Kahr* and Stephanie S. Lee*

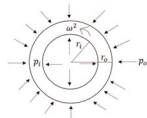


13737

COMPARATIVE ANALYSIS OF STEADY STATE CREEP IN SUS-ZrO₂ AND Al-ZrO₂ FUNCTIONALLY GRADED PRESSURIZED CYLINDERS WITH ITS IMPLICATIONSSahni et al., 2025 | *Nanoscale*

BACKGROUND
Secondary Creep Analysis in Rotating Anisotropic Functionally Graded Cylinder (axisymmetric) Under Internal/External Pressure.

MATERIAL AND METHOD
Functionally Graded Material. Exponential Volume Reinforcement of ZrO₂ in SUS and Al Metal Matrix. Closed Form Analytical Solution Using Norton's Creep Law.



RESULT 3
Al-ZrO₂ FG cylinder is superior because it manages stress more efficiently, resists creep deformation better, and enhances long-term durability.

RESULT 1
Al-ZrO₂ FG cylinder undergoes a lower tangential creep strain rate under an external pressure compared to the SUS-ZrO₂ FG cylinder.

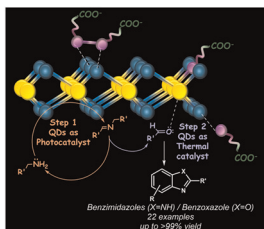
RESULT 2
Al-ZrO₂ FG cylinder has lower creep strain rates in the radial direction at the outer radius under external pressure. This helps in minimizing deformation caused by angular body force, which is crucial for maintaining structural integrity over time.

CONCLUSION
Al-ZrO₂ FG cylinder appears to be the more convenient choice compared to the SUS - ZrO₂ FG cylinder for applications involving external pressure and angular body force.

Comparative analysis of steady-state creep in SUS-ZrO₂ and Al-ZrO₂ functionally graded pressurized cylinders and its implications

Manoj Sahni,* Parth Dinesh Mehta and Sandeep Kumar Paul

13746

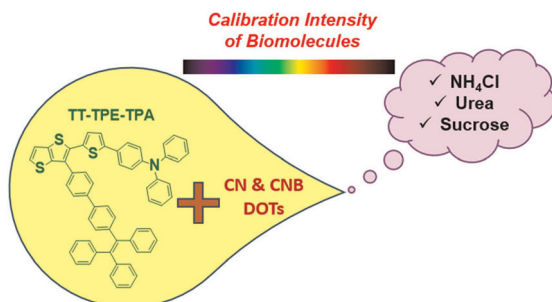


- ✓ Facile protocol for generation of a diverse range of bioactive benzimidazoles/benzoxazole.
 - ✓ Application of surface-engineered TMD as bifunctional catalyst.
- ✓ Reusable, economical and easy-to-prepare catalyst.
 - ✓ Benign reaction conditions.
- ✓ Nanocatalyst mediates the formation of active ingredients *in situ*.

Thiolated molybdenum diselenide quantum dots as a bifunctional catalyst towards the synthesis of benzimidazoles

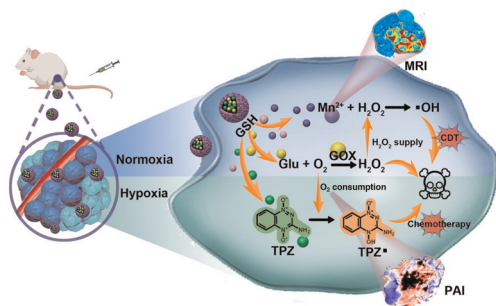
Komal Jaiswal, Rushikesh Jagtap and Mrinmoy De*

13756

Thienothiophene-based quantum dots: calibration of photophysical properties *via* carbon dot and biomolecular interactions

Recep Isci,* Ozge Ibis, Garen Suna, Caner Unlu* and Turan Ozturk*

13767



Smart self-assembly of a multifunctional theranostic nanozyme for self-enhanced precise chemo/chemodynamic therapy

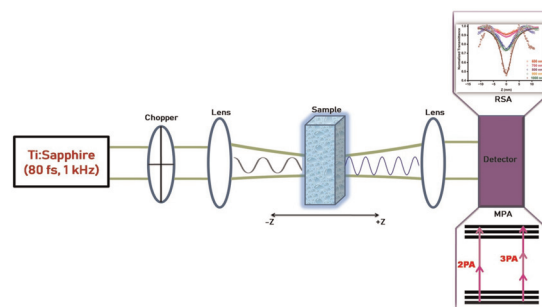
Jin Tao, Junhui Wei, Junnan Kan, Kai Qi, Tingting Wang, Ailing Wang, Wenxin Pei, Haiyan Gao, Caixia Yang* and Xianglin Li*



13777

Broadband laser protection and enhanced nonlinear optical response of samarium–metal–organic framework-based white/black carbon hybrids

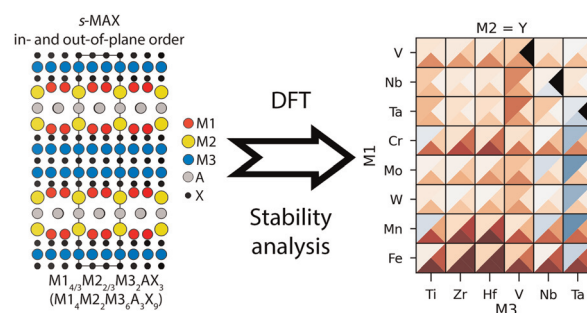
M. Saravanan,* Vinod K. Rajput, K. Suresh, Sri Ram G. Naraharisetty, Sajan D. George, I. Vetha Potheher,* Marek Brzeziński and B. N. Vedha Hari



13787

Combined in- and out-of-plane chemical ordering in super-ordered MAX phases (s-MAX)

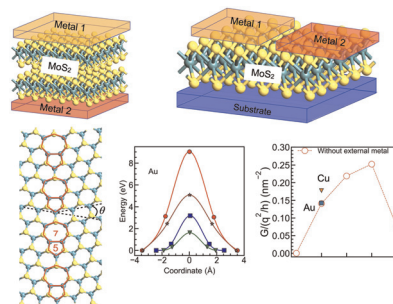
Martin Dahlqvist* and Johanna Rosen*



13797

Effect of grain boundaries on metal atom migration and electronic transport in 2D TMD-based resistive switches

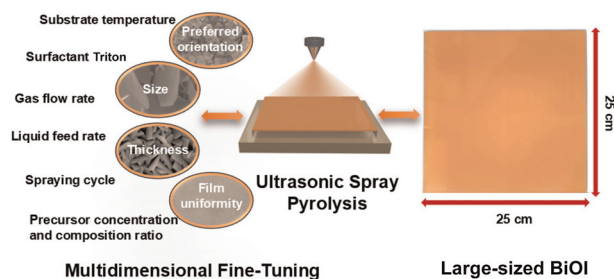
Mohit D. Ganeriwala,* Daniel Luque-Jarava, Francisco Pasadas, Juan J. Palacios, Francisco G. Ruiz, Andres Godoy* and Enrique G. Marin



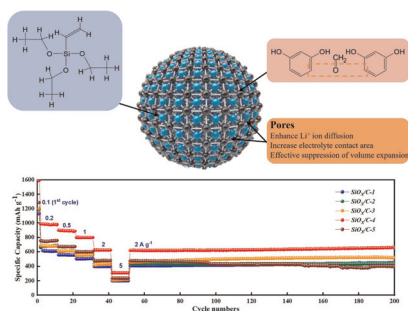
13808

Enabling multidimensional fine-tuning of large-sized BiOI films using ultrasonic spray pyrolysis

Hao Wang, Weilong Qin, Qitao Liu, Neway Belachew, Jianming Li, Qinglu Liu, Jiabo Le and Yongbo Kuang*



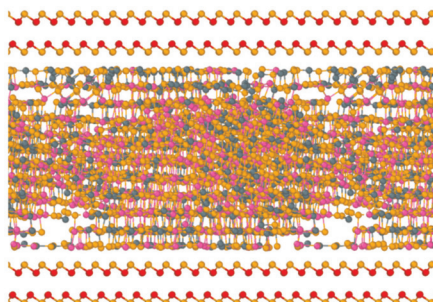
13818



SiO_x/C composite spheres as an anode material for high-performance lithium-ion batteries

Ho Jin Yoo, Eun Mi Kim* and Sang Mun Jeong*

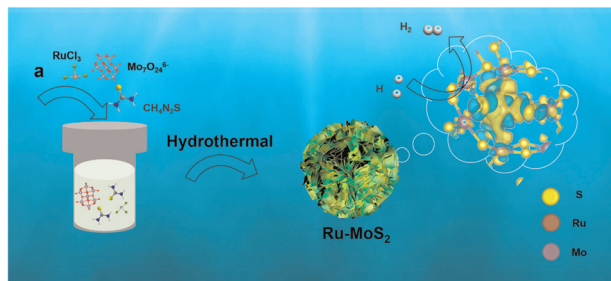
13828



Simulation of the crystallization process of Ge₂Sb₂Te₅ nanoconfined in superlattice geometries for phase change memories

Debdipto Acharya, Omar Abou El Kheir, Simone Marcorini and Marco Bernasconi*

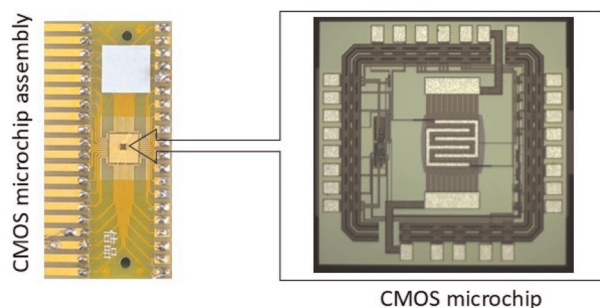
13842



Ru doping induces phase transition and in-plane S-site electronic modulation in ternary MoS₂ heterostructures to enhance hydrogen evolution in water/seawater

Jianpeng Sun, Jianan Rao, Shiyu Qin, Xiang Li, Ru Jia, Kelei Huang, Yu Zheng and Xiangchao Meng*

13850



Low temperature inkjet-printed metal oxide sensors for sensitive and selective NO₂ detection

P. K. Shihabudeen, Shivam Gupta, Yu-Hsien Lin, Shih-Wen Chiu, Yu Ting Chuang, Yuan Fu Tang, Nyan-Hwa Tai and Kea-Tiong Tang*

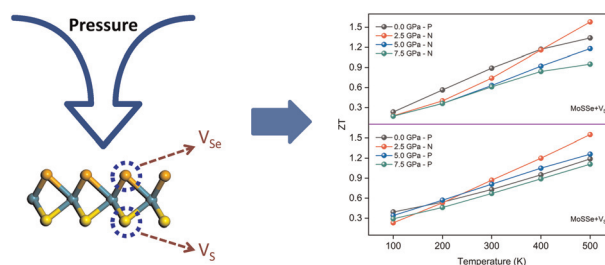


PAPERS

13861

Effect of pressure on the thermoelectric performance of monolayer Janus MoSSe materials with different native vacancy defects

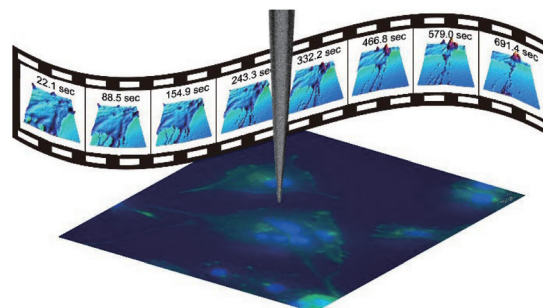
Yuan Shang, Xiaopeng Pan, Yanxing Jia, Yuqiang Wu and Mengtao Sun*



13869

Nanoscale structural dynamics of cell edges in breast tumour cells revealed by scanning ion conductance microscopy

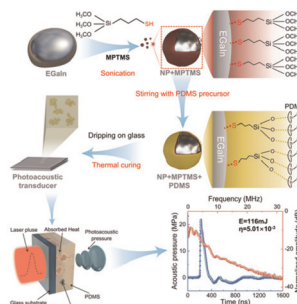
Masahiro Yamazaki, Linhao Sun, Tatsunori Nishimura, Tsunaki Hongu, Shigeyuki Takamatsu, Toshifumi Gabata, Noriko Gotoh* and Shinji Watanabe*



13880

High-efficiency photoacoustic transducers based on plasmonic EGaIn liquid metal nanoparticles

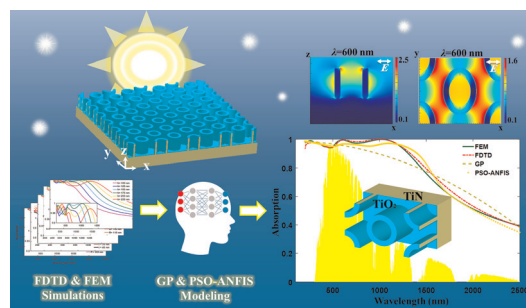
Cheng Luo, Rui Zhou, Yihao Li, Min Li, Xiaoyan Wen, Ming-Yu Li, Shuo Deng, Sisi Liu, Hongyun Gao* and Haifei Lu*



13888

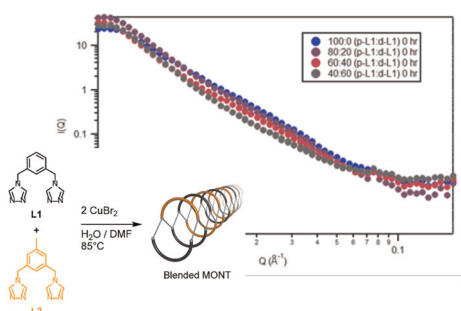
Machine-learning-empowered FDTD/FEM simulations for predictive solar energy absorption in plasmonic metamaterial nanocavity arrays

Zahra Ashrafi-Peyman, Amir Dashti, Amir Jafargholi, John L. Zhou* and Alireza Z. Moshfegh*



PAPERS

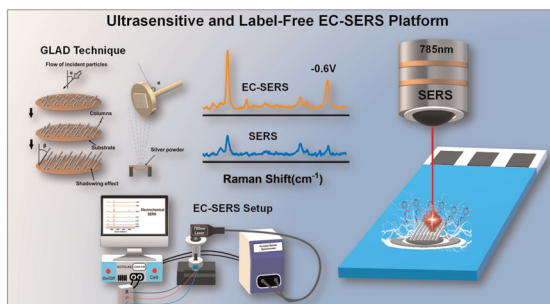
13905



Insights into the copolymerization of metal–organic nanotubes from ligand mixtures using small angle neutron scattering

Md Ashraful Haque, Jacob A. Barrett, Xian B. Carroll, David M. Jenkins* and Mark D. Dadmun*

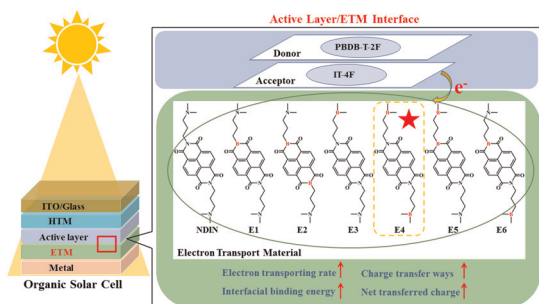
13915



Potential-modulated SERS profiling via GLAD-fabricated Ag nanorod arrays for ultrasensitive and label-free spectroelectrochemical sensing

Lakshay Bhardwaj, Jyoti Yadav and J. P. Singh*

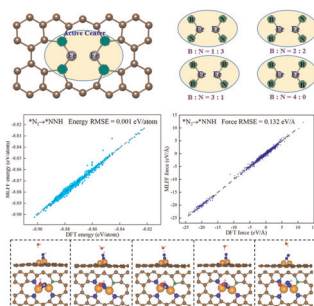
13929



Boron-containing electron transport materials based on naphthalene diimide for organic solar cells: a theoretical study

Shu-Pu Yao, Jie Yang,* Qian Guo, Xiao-Juan Yang and Quan-Song Li*

13939



Exploring dual-iron atomic catalysts for efficient nitrogen reduction: a comprehensive study on structural and electronic optimization

Zhe Zhang,* Wenxin Ma, Jiajie Qiao, Xiaoliang Wu, Shaowen Yu, Weiye Hou, Xiang Huang, Rubin Huo, Hongbo Wu* and Yusong Tu*



13951

Cuticular proteins (crusticuls) affect 3D chitin bundle nanostructure

Shai A. Shaked, Simy Weil, Rivka Manor, Eliahu D. Aflalo, Sharon Moscovitz, Nitzan Maman, Raquel Maria, Benjamin Kruppke, Thomas Hanke, Jerry Eichler, Barak Ratzker, Maxim Sokol and Amir Sagi*

